

Image And Pixel Based Scheme For Bleeding Detection In Wireless Capsule Endoscopy Images

Vani V. and K.V.Mahendra Prashanth

Abstract Bleeding detection techniques that are widely used in digital image analysis can be categorized in 3 main types: image based, pixel based and patch based. For computer-aided diagnosis of bleeding detection in Wireless Capsule Endoscopy (WCE), the most efficient choice among these remains still a problem. In this work, different types of Gastro intestinal bleeding problems: Angiodysplasia, Vascular ectasia and Vascular lesions detected through WCE are discussed. Effective image processing techniques for bleeding detection in WCE employing both image based and pixel based techniques have been presented. The quantitative analysis of the parameters such as accuracy, sensitivity and specificity shows that YIQ and HSV are suitable color models; while LAB color model incurs low value of sensitivity. Statistical based measurements achieves higher accuracy and specificity with better computation speed up as compared to other models. Classification using K-Nearest Neighbor is deployed to verify the performance. The results obtained are compared and evaluated through the confusion matrix.

1 Introduction

Capsule endoscopy has been proved as a standard well-established non-invasive technique for identification of obscure Gastro Intestinal (GI) bleeding. The standard method for reading capsule endoscopy images involves watching streams of 50,000 capsule endoscopy images; it is time consuming; requiring about 17-60 minutes of average reading time[1]. An important challenge in the area of capsule endoscopy is

Vani V.

SJB Institute of Technology, Visvesvaraya Technological University, Bengaluru 560060, India, e-mail: vaniv81@gmail.com

K.V.Mahendra Prashanth

SJB Institute of Technology, Visvesvaraya Technological University, Bengaluru 560060, India e-mail: kvmprashanth@sjbit.edu.in

identification and detection of obscure GI bleeding. Suspected Blood Identification system (SBIS) developed by the capsule manufacture has reported to provide false alarm rates with sensitivity in the range of 30%-80% [2].

Vascular Ectasias, Vascular lesions and Angiodysplasia are the major bleeding disorders in the GI tract[3]. Angiodysplasia is the second leading cause of bleeding in lower GI tract in patients older than 60 years; and the most common vascular abnormality of GI tract [4]. Vascular ectasias [4] is a rare but significant cause of lower GI bleeding in elderly of age group 60 years.

The three classical methods for bleeding detection are based on image, pixel and patch. Image based detection use various features of image such as statistical features and color similarity for bleeding detection [6, 7]. Since the image based features works on the whole image, it is much faster but provides poor performance. While pixel based detection relies on bleeding detection pixel wise based on neural network, thresholding and color features [8],[9],[10]. This method provides better classification but high computational cost. The patch based method provides a trade-off between performance and speed. In this method the images are divided into patches/blocks through methods such as LBP (Local Binary Pattern) and the most informative patches are further used for classification [11, 12].

This paper describes the design and implementation of image based and pixel based methodology to detect bleeding in WCE images. The image based techniques employed are color model, histogram and statistical based measurements. The pixel based measurements employed is the color range ratio through thresholding technique. The study on bleeding detection techniques reveals the various possibilities through which bleeding can be detected; yet there exists various trade-offs in metrics such as sensitivity and specificity. Hence an effort to provide a quantitative comparison of these methods have been employed in this paper; thus providing a simple and efficient choice of these methods. The experiments were carried out on several WCE images consisting of normal images and various types of bleeding images collected from Endoatlas image database [13].

2 Image Based - Color Model

Since medical experts differentiate bleeding from non-bleeding based on color information; choosing an appropriate color model is very critical; that investigates which color model would be efficient for the computer program to extract the color information. This study aims at investigation of commonly used colors (RGB, CIELAB and YIQ) to enable the usage of computationally and conceptual simple bleeding detection methods [15].

It is observed that second component of CIE Lab color space and YIQ provides better identification of bleeding region [16, 17]. Further HSI color model proved to be an ideal tool for further image processing and classification of bleeding anomaly; since HSI color space is much closer to human perception than any other domain. Hue is a color attribute which describes the pure color. Saturation is a relative color

purity i.e lack of white color. Intensity is the brightness. Maximum intensity corresponds to pure white and minimum intensity corresponds to pure black.

The YIQ model is designed originally to separate chrominance from luminance. Y component contains luminance or intensity component, while I and Q components contain color information [18]. The conversion equation is quite simple to implement. The RGB to YIQ color conversion were done as follows:

$$Y = 0.3 \times R + 0.59 \times G + 0.11 \times B; \quad (1)$$

$$I = 0.6 \times R - 0.28 \times G - 0.32 \times B; \quad (2)$$

$$Q = 0.21 \times R - 0.52 \times G + 0.31 \times B; \quad (3)$$

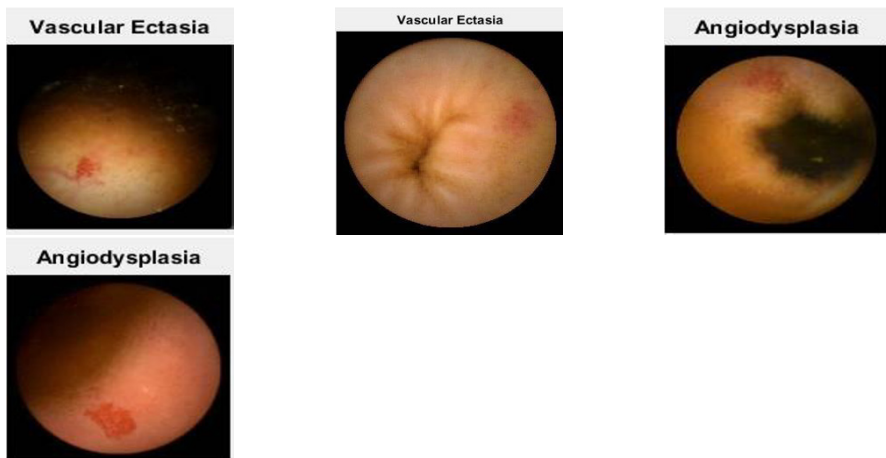


Fig. 1 Original Images a.Vascular Ecstasia b. Vascular Ecstatia c.Angiodysplasia d. Angiodysplasia [13]

The original WCE images of size 150 * 150 pixels and resolution 75(horizontal) * 75(vertical) dpi obtained from Endoatlas image database [13] for bleeding disorders such as Vascular ectasia and Angiodysplasia are shown in Fig 1. Fig 2 shows the same images after color conversion to YIQ color space. It is evident that bleeding region is more prominent in YIQ color space as compared to the original images shown in Fig 1 [13].

CIELAB color space is a color opponent space; L represents the lightness and A and B represents the color opponent dimensions. Color conversion from RGB to CIELAB color space for the second component of LAB color space is shown in Fig 3; indicating that A channel has the tendency in separating the non-informative regions from informative(i.e bleeding) region [14]

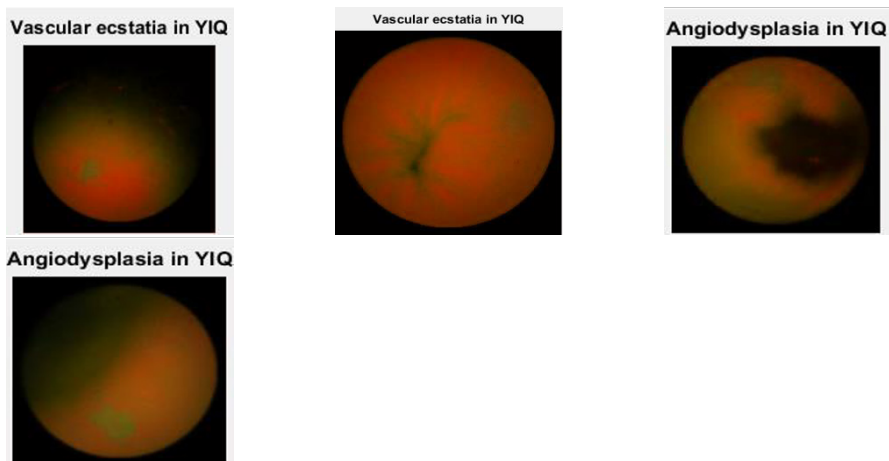


Fig. 2 After color conversion to YIQ a.Vascular Ecstasia b. Vascular Ecstasia c.Angiodysplasia d. Angiodysplasia

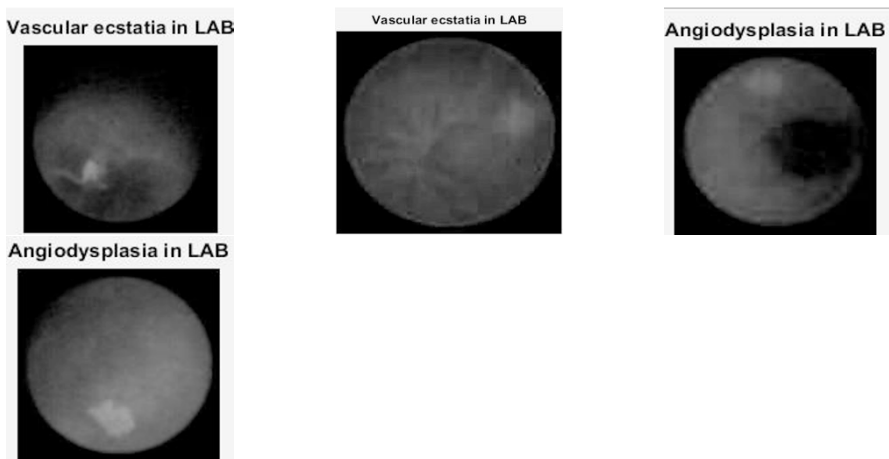


Fig. 3 After color conversion to LAB a.Vascular Ecstasia b. Vascular Ecstasia c.Angiodysplasia d. Angiodysplasia

To convert RGB to LAB color space, it is important to determine an absolute color space for RGB since RGB is not an absolute color space. The standard technique to convert RGB to standard color space XYZ is shown in equations(4)-(6)

$$[X] = [[-3.240479 \quad -1.537150 \quad -0.498535] \times [R]] \tag{4}$$

$$[Y] = [[-0.969256 \quad 1.875992 \quad 0.041556] \times [G]] \tag{5}$$

$$[Z] = [[0.055648 \quad -0.204043 \quad 1.057311] \times [B]] \quad (6)$$

The color conversion from XYZ to LAB color space can be done as shown in equations (7)-(9)

$$CIEL = \left(116 \times \left(\frac{X}{X'} \right) - 16 \right) \quad (7)$$

$$CIEA = 500 \times \left(\left(\frac{X}{X'} \right) - \left(\frac{Y}{Y'} \right) \right) \quad (8)$$

$$CIEB = 200 \times \left(\left(\frac{Y}{Y'} \right) - \left(\frac{Z}{Z'} \right) \right) \quad (9)$$

where X', Y' and Z' are tristimulus values of LAB color space

3 Pixel Based Color Range Ratio

The color descriptor based on range ratio color of RGB pixel values was evaluated. The range ratio were evaluated for every pixel [19]. The goal is to segregate the bleeding pixel from non bleeding pixel through the pixel value. Segregation of bleeding pixels through purity of bleeding color (R=255;G=0;B=0) failed to identify many bleeding regions as shown in Fig 4. Hence every pixel was investigated to develop a threshold value for bleeding pixel. Two variations of the color range ratio detection methods are proposed; first method for exact blood color detection and second method for more tolerant identification of colors close to bleeding. The investigation required bleeding pixel to have the range of values for R,G,B as follows: $((R \leq 177 \& R \geq 215) \& (G \leq 99 \& G \geq 56) \& (B \leq 52 \& B \geq 20))$. The results obtained through color range ratio are obtained as shown in Fig.4. The experimental evaluation leads to satisfactory results.

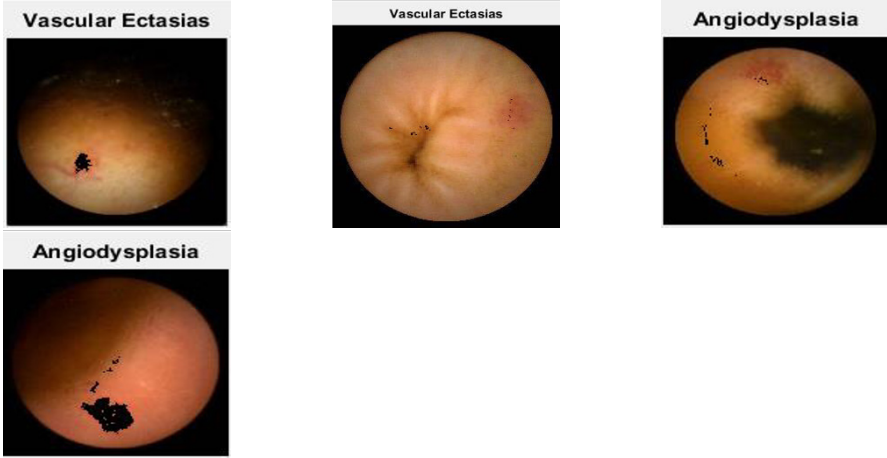


Fig. 4 Pixel based bleeding detection using range ratio color a.Vascular Ecstasia b. Vascular Ecstasia c.Angiodysplasia d. Angiodysplasia

4 Pixel Based - Color Similarity Measurement

A color similarity technique to measure the similarity between a pixel in RGB to a known typical bleeding pixel is employed. Lower the color similarity, lesser is the similarity between the two pixels; higher the color similarity, higher is the similarity between two pixels[25].

The color similarity is estimated through closeness of pixel values between $P(R,G,B)$ and $P0(R0,G0,B0)$ where $P(R,G,B)$ is the color vector of the pixel being tested and $C0(R0,G0,B0)$ is the known typical bleeding pixel. The similarity of color vector depends on amplitude and direction similarity. The amplitude similarity between $P(R,G,B)$ and $P0(R0,G0,B0)$ is measured by absolute value of difference $|P| - |P0|$. The coefficient of amplitude similarity is obtained as given in equation (10)

$$n = 1 - \frac{(|P| - |P0|)}{|P0|}; \quad (10)$$

$$|P| = \sqrt{R^2 \times G^2 \times B^2}; \quad (11)$$

$$|P0| = \sqrt{R0^2 \times G0^2 \times B0^2}; \quad (12)$$

Equation (10) shows that when $|P| = |P0|$, coefficient of amplitude similarity n is equal to 1. Higher the value of n , higher is the similarity and vice versa.

The direction similarity between the pixels shown in Fig. 5 is measured by the angle α computed as

$$\cos \alpha = \frac{P \times P0}{|P|/times|P0|} = \frac{R \times R0 + G \times G0 + B \times B0}{(\sqrt{R^2 + G^2 + B^2}) \times \sqrt{(R0^2 + G0^2 + B0^2)}} \tag{13}$$

Smaller the value of α , larger is the function value of $\cos\alpha$ and more similar are the directions of color vectors. The pixel value is calculated as bleeding pixel, non-bleeding pixel or suspected bleeding based on following function.

$$\begin{aligned} \text{Output}(X) &= \{ \text{Bleeding}; \text{if } G(X) \& C(X) = 1 \\ &\quad \text{Non - Bleeding}; \text{if } G(X) \parallel C(X) = 0 \\ &\quad \text{SuspectedBleeding}; \text{others} \end{aligned}$$

where $\&$ represents logical AND operation and \parallel represents logical OR operation.

$G(X)$ is the gray intensity similarity coefficient and $C(X)$ is the chroma similarity coefficient respectively.

$$\begin{aligned} G(X) &= \{ \text{1 if } d(X) \geq 0 \\ &\quad \text{0 if } d(X) < 0 \end{aligned}$$

$d(X)$ is the classifying function given as $d(X) = n - n_{min}$ where n_{min} is the threshold value of similarity co-efficient chosen as 0.96

$$\begin{aligned} C(X) &= \{ \text{1 if } d_C(X) \geq 0 \\ &\quad \text{0 if } d_C(X) < 0 \end{aligned}$$

where $d_C(X) = \cos \alpha - \cos \alpha_{min}$

where $\cos \alpha_{min} = 0.96$

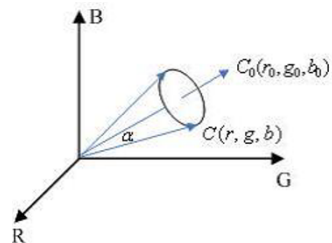


Fig. 5 Color vector similarity measurement [25]

The results obtained through color similarity measurement shown in Fig 6 shows that possibilities of suspected bleeding is more in darker areas; hence increasing the number of false positive cases, thereby decreasing specificity .Thus decreasing the ability of the system to correctly identify the non-blood frame.

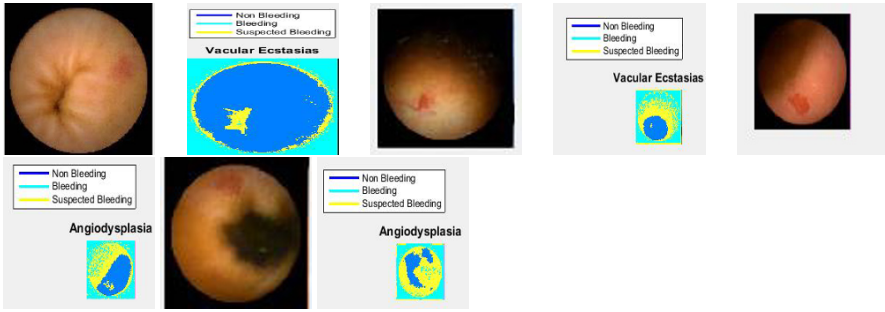


Fig. 6 Color similarity based bleeding detection a.Vascular Ecstasia b. Vascular Ecstasia c.Angiodysplasia d. Angiodysplasia

5 Statistical Measures for RGB Color Plane

A very effective technique to search for most similar images out of huge database is Content Based Image Retrieval (CBIR) system [21]; which proves to be beneficial for WCE due to its huge image database. Hence statistical features obtained from the colour histogram are tested to detect and delineate bleeding regions from set of capsule endoscopy images.

Colour is an important cue for medical experts to identify different regions in an image. Hence it is suitable to employ colour features for extraction. In the colour images, colour distribution of each plane is modelled by its individual histogram. Statistical based measures like mean, variance, standard deviation, entropy and skew of first order colour histograms are statistical indicators that categorize various properties of images.

1. Mean of an image provides the average brightness of an image
2. Variance of an image provides information on distribution of the pixel intensities around mean intensity value. Higher value of variance indicates higher contrast
3. Standard Deviation is the square root of variance. It provides information about contrast
4. Skew measures the asymmetry about the mean in the intensity level distribution. A positive value of skew indicates histogram distribution has a longer tail towards the left; a negative value of skew indicates histogram distribution has longer tail towards the right
5. Entropy is a measure of information content or uncertainty. Images where pixel values change unexpectedly, have large entropy values
6. Kurtosis is the relative flatness or peakness of a distribution compared to normal distribution
7. Moment is the distribution of random variable about its mean. Higher order moments are related to spread and shape of the distribution

The above statistical parameters were applied on the R/G intensity ratio domain to determine the features for bleeding. The behavior of each statistical parameter were investigated for bleeding and non-bleeding images.

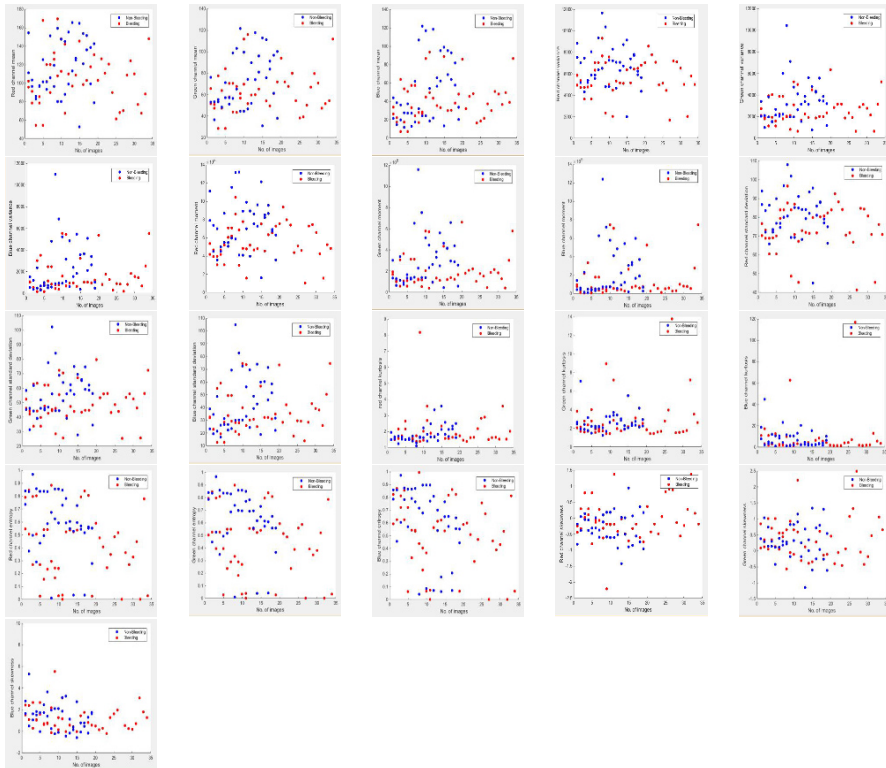


Fig. 7 Scatter plot of bleeding and non-bleeding images in RGB domain (a)Mean of Red channel (b)Mean of Green channel (c)Mean of Blue channel (d)Variance of red channel (e)Variance of Green channel (f)Variance of Blue channel (g)Moment of Red channel (h)Moment of Green channel (i)Moment of Blue channel (j)Standard deviation of Red channel (k)Standard deviation of Green channel (l)Standard deviation of Blue channel (m)Kurtosis of Red channel (n)Kurtosis of Green channel (o)Kurtosis of Blue channel (p)Entropy of Red channel (q)Entropy of Green channel (r)Entropy of Blue channel (s)Skewness of Red channel (t)Skewness of Green channel (u)Skewness of Blue channel(Red scatter plots indicate bleeding images;Blue scatter plots indicate non-bleeding images)

The scatter plots show that only selective feature combinations produce differentiable cases of bleeding and non-bleeding.

The investigation of statistics in Fig 7 reveals that presence of bleeding region lowers the value of mean, moment, variance and standard deviation distribution as compared to non-bleeding images. However there is a certain degree of overlap between the two classes. Certain statistical measures shows relatively higher value for

entropy, kurtosis and skew; measured for bleeding disorders such as colon carcinoma and colonic polyps with bleeding.

6 Histogram Probability Distribution and Statistical Measures for HSV Color Plane

Though RGB colour space is most widely used in bleeding detection; one problem with RGB colour space is it contains colour information and colour intensity. Hence, it is difficult to identify the colour from an individual RGB colour component. The HSV colour scheme is much closer to conceptual human understanding of colours and hence widely used in computer vision application. It has the ability to separate achromatic and chromatic components. The RGB to HSV colour transformation is initially done and then the statistical measures such as mean, variance and moment are calculated for hue, saturated and value plane individually [22, 23, 24]. The statistical measures such as mean, variance, moment, standard deviation, entropy and skewness has been computed for HSV plane individually and scatter plot has been obtained as shown in Fig 8.

The behavior of each statistical measure of non-bleeding and bleeding images is investigated. A combination of different statistical parameters is studied through the aid of KNN classifier for identification of bleeding from non-bleeding images.

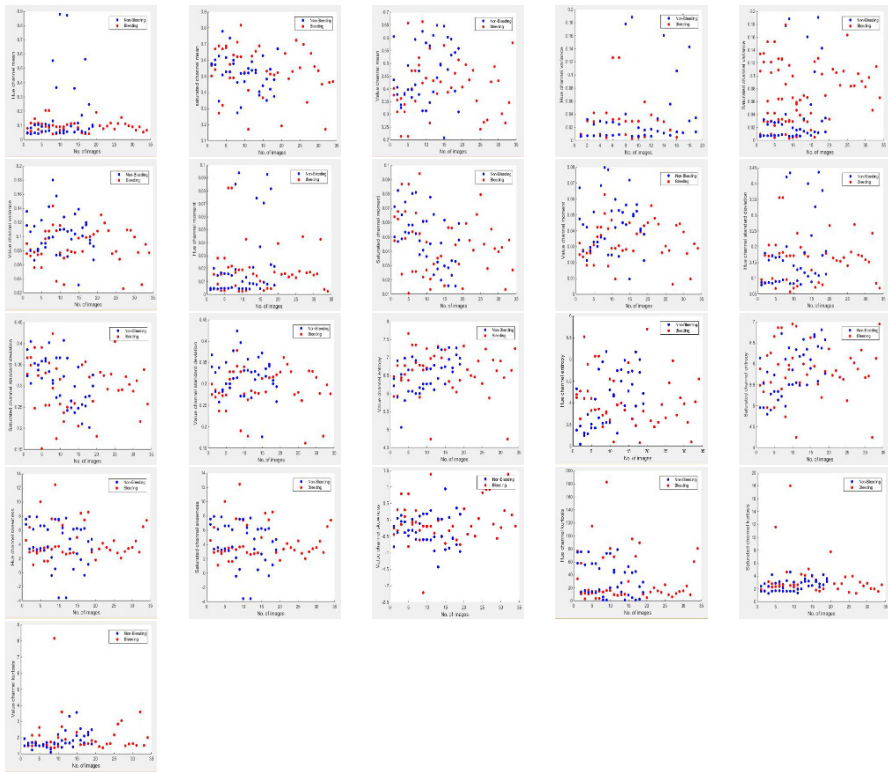


Fig. 8 Scatter plot of bleeding and non-bleeding images in HSV domain (a)Mean of hue channel (b)Mean of saturated channel (c)Mean of value channel (d)Variance of hue channel (e)Variance of saturated channel (f)Variance of value channel (g)Moment of hue channel (h)Moment of saturated channel (i)Moment of value channel (j)Standard deviation of hue channel (k)Standard deviation of saturated channel (l)Standard deviation of value channel (m)Entropy of hue channel (n)Entropy of saturated channel (o)Entropy of value channel (p)Skewness of hue channel (q)Skewness of saturated channel (r)Skewness of value channel (s)Kurtosis of hue channel (t)Kurtosis of saturated channel (u) Kurtosis of value channel(Red scatter plots indicate bleeding images;Blue scatter plots indicate non-bleeding images)

7 K Nearest Neighbor KNN Classifier

The KNN classifier based on Leave-One-Out cross validation technique for k=1 was adopted for classification of bleeding and non-bleeding images and performance was compared. KNN classifier was used for all different combination of statistical features calculated in the HSV and RGB plane. The results obtained through KNN classifiers is tabulated in Table 1.

8 Results & Discussion

Experimental evaluation was conducted on 61 bleeding images and 38 normal images. The image under test is identified as True Positive (TrP) when the system and medical expert consider as abnormal; True Negative (TrN): when the system and medical expert consider the image as normal; False Positive (FaP): when the test image is identified as normal by medical expert but abnormal by the system and False Negative (FaN): when the image is identified as abnormal by expert and normal by system.

The performance of the bleeding detection algorithms have been accessed through following parameters: sensitivity, specificity and accuracy which are computed as shown in equations (17-19). The ability of the system to correctly identify the image as abnormal is a measure of sensitivity; while the ability of the system to correctly classify the image as normal is a measure of specificity. The overall performance of the system is measured through accuracy.

$$sensitivity = \frac{\sum(TrP)}{(\sum(TrP) + \sum(FaN))} \tag{14}$$

$$specificity = \frac{\sum(TrN)}{(\sum(TrN) + \sum(FaP))} \tag{15}$$

$$accuracy = \frac{\sum(TrP) + \sum(TrN)}{\sum(TrP) + \sum(TrN) + \sum(FaP) + \sum(FaN)} \tag{16}$$

The computation speed of the algorithms was computed in seconds.

Table 1 Comparative Evaluation of Performance

| Method | Algorithm | Accuracy(%) | Sensitivity(%) | Specificity(%) | Computation time(seconds) |
|-------------|------------------------------|-------------|----------------|----------------|---------------------------|
| Image Based | YIQ Color model | 70.7 | 92.85 | 43.9 | 30.743 |
| Image Based | LAB Color model | 57.57 | 49.09 | 68.18 | 30.743 |
| Image Based | Statistical measures(RGB)* | 80.8 | 88.52 | 68.42 | 27.875 |
| Image Based | Statistical measures(HSV)* | 82.82 | 90.3 | 66.67 | 30.6875 |
| Image Based | Statistical measures(HSV)** | 78.78 | 83.87 | 70.3 | 27.0313 |
| Image Based | Statistical measures(HSV)*** | 80.80 | 90.3 | 64.86 | 13.0938 |
| Pixel Based | Color range ratio | 73.73 | 77.61 | 65.6 | 16.743 |
| Pixel Based | Color Similarity | 52.52 | 91.89 | 36 | 233.862 |

(*indicates all statistical measures **indicates entropy,skew,kurtosis ***mean,variance and moment)

The graphical representation of comparative evaluation is shown in Fig 9 which depicts a precise graphical comparison among the various methods.

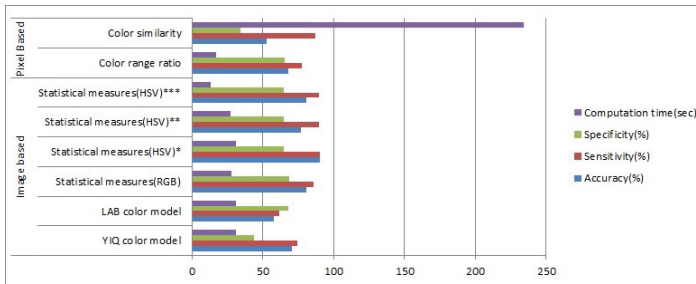


Fig. 9 Graphical representation of comparative evaluation performance (*indicates all statistical measures **indicates entropy,skew,kurtosis only ***mean,variance and moment only)

Statistical based measurement for HSV color space for all statistical measures provides superior accuracy of 89.89% with superior sensitivity of 90.3%; while statistical based measurement for RGB color space achieves the best specificity of 68.42%. As observed, pixel based measurement required an appreciable computation time; whereas statistical based measurements consumed very less computation time.

However, having a higher value of sensitivity or specificity remains a matter of debate. In bleeding detection physician may prefer to have more false positive hit; but more number of false positives can also be annoying. The low value of sensitivity for LAB color model is due to the more number of false negatives; as the system was unable to recognize faint traces of bleeding in the images.

The performance metrics are represented with the help of a confusion matrix as shown in Table 2.

Table 2 Confusion Matrix

| Algorithm | #TP | #TN | #FP | #FN |
|------------------------------|-----|-----|-----|-----|
| YIQ Color model | 52 | 18 | 23 | 4 |
| LAB Color model | 27 | 30 | 14 | 28 |
| Statistical measures(RGB)* | 54 | 26 | 12 | 7 |
| Statistical measures(HSV)* | 56 | 24 | 13 | 6 |
| Statistical measures(HSV)** | 52 | 26 | 11 | 10 |
| Statistical measures(HSV)*** | 56 | 24 | 13 | 6 |
| Color range ratio | 52 | 21 | 11 | 15 |
| Color similarity | 34 | 18 | 32 | 3 |

(*indicates all statistical measures **indicates entropy,skew,kurtosis only ***mean,variance and moment only)

9 Conclusion

In this paper, image and pixel based method for detection of bleeding disorders in Wireless Capsule Endoscopy images is carried out. The results of image based techniques and pixel based techniques are compared and evaluated. The experimental results shows that statistical based measurement was able to achieve high accuracy and specificity with better computation speed up as compared to other image and pixel based techniques. The experiment also reveals that YIQ and HSV are suitable colour model as they show higher accuracy, sensitivity and specificity as compared to LAB color space.

To summarize image based methods failed to identify small bleeding regions; thereby resulted in poor performance but faster computation time. Pixel based methods suffered from higher trade-off between sensitivity and specificity and large computation time.

The future work is aimed at patch based bleeding detection techniques and to reduce the trade-off between sensitivity and specificity. Further, research needs to be carried out to improve the overall accuracy, sensitivity and specificity through use of better features and classifiers.

Acknowledgements We would like to thank Dr.Anand Dotihal , Gastroenterologist, Bangalore for his valuable medical guidance on the different bleeding disorders in numerous images.

References

1. Stein, Adam C., et al. "A Rapid and Accurate Method to Detect Active Small Bowel Gastrointestinal Bleeding on Video Capsule Endoscopy." *Digestive diseases and sciences* 59.10 (2014): 2503-2507.
2. Choi, Hyuk Soon, et al. "The sensitivity of suspected blood indicator (SBI) according to the background color and passage velocity of capsule endoscopy." *JOURNAL OF GASTROENTEROLOGY AND HEPATOLOGY*. Vol. 25. COMMERCE PLACE, 350 MAIN ST, MALDEN 02148, MA USA: WILEY-BLACKWELL, 2010.
3. Hara, Amy K., et al. "Small Bowel: Preliminary Comparison of Capsule Endoscopy with Barium Study and CT 1." *Radiology* 230.1 (2004): 260-265.
4. Gunjan, Deepak, et al. "Small bowel bleeding: a comprehensive review." *Gastroenterology report* (2014): gou025.
5. Nguyen, Hien, Connie Le, and Hanh Nguyen. "Gastric Antral Vascular Ectasia (Watermelon Stomach)—An Enigmatic and Often-Overlooked Cause of Gastrointestinal Bleeding in the Elderly." *Issues* 2016 (2016).
6. Ghosh, T., et al. "An automatic bleeding detection scheme in wireless capsule endoscopy based on statistical features in hue space." *Computer and Information Technology (ICCIT), 2014 17th International Conference on*. IEEE, 2014.
7. Guobing, P. A. N., X. U. Fang, and C. H. E. N. Jiaoliao. "A novel algorithm for color similarity measurement and the application for bleeding detection in WCE." *International Journal of Image, Graphics and Signal Processing* 3.5 (2011): 1.
8. Pan, Guobing, et al. "Bleeding detection in wireless capsule endoscopy based on probabilistic neural network." *Journal of medical systems* 35.6 (2011): 1477-1484.

9. Bourbakis, N., Sokratis Makrogiannis, and Despina Kaviraki. "A neural network-based detection of bleeding in sequences of WCE images." *Bioinformatics and Bioengineering*, 2005. BIBE 2005. Fifth IEEE Symposium on. IEEE, 2005.
10. Poh, Chee Khun, et al. "Multi-level local feature classification for bleeding detection in wireless capsule endoscopy images." *Cybernetics and Intelligent Systems (CIS)*, 2010 IEEE Conference on. IEEE, 2010.
11. Lau, Phooi Yee, and Paulo Lobato Correia. "Detection of bleeding patterns in WCE video using multiple features." *Engineering in Medicine and Biology Society*, 2007. EMBS 2007. 29th Annual International Conference of the IEEE. IEEE, 2007.
12. Fu, Yanan, Mrinal Mandal, and Gencheng Guo. "Bleeding region detection in WCE images based on color features and neural network." *Circuits and Systems (MWSCAS)*, 2011 IEEE 54th International Midwest Symposium on. IEEE, 2011.
13. Atlas of Gastrointestinal Endoscopy. 1996 [online]. Available: <http://www.endoatlas.com/index.html>
14. Hunter Labs (1996). "Hunter Lab Color Scale". *Insight on Color* 8 9 (August 1-15, 1996). Reston, VA, USA: Hunter Associates Laboratories
15. Sharma, Gaurav, and H. Joel Trussell. "Digital color imaging." *Image Processing, IEEE Transactions on* 6.7 (1997): 901-932
16. J. Schanda, *Colorimetry: Understanding the CIE system*: Wiley. com, 2007
17. Szczypiski, Piotr, et al. "Texture and color based image segmentation and pathology detection in capsule endoscopy videos." *Computer methods and programs in biomedicine* 113.1 (2014): 396-411
18. Hughes, John F., et al. *Computer graphics: principles and practice*. Pearson Education, 2013
19. Al-Rahayfeh, Amer A., and Abdelshakour A. Abuzneid. "Detection of bleeding in wireless capsule endoscopy images using range ratio color." *arXiv preprint arXiv:1005.5439* (2010).
20. Ghosh, T., et al. "An automatic bleeding detection scheme in wireless capsule endoscopy based on histogram of an RGB-indexed image." *Engineering in Medicine and Biology Society (EMBC)*, 2014 36th Annual International Conference of the IEEE. IEEE, 2014
21. Sergyan, S., *Color histogram features based image classification in content-based image retrieval systems* In: *Applied Machine Intelligence and Informatics*, 2008. SAMI 2008. 6th International Symposium on, pp. 221224, 2008
22. Ghosh, T., et al. "An automatic bleeding detection scheme in wireless capsule endoscopy based on statistical features in hue space." *Computer and Information Technology (ICCIT)*, 2014 17th International Conference on. IEEE, 2014
23. Shah, Subodh K., et al. "Classification of bleeding images in wireless capsule endoscopy using HSI color domain and region segmentation." *URI-NE ASEE 2007 Conference*. 2007
24. Ghosh, Tonmoy, et al. "A statistical feature based novel method to detect bleeding in wireless capsule endoscopy images." *Informatics, Electronics & Vision (ICIEV)*, 2014 International Conference on. IEEE, 2014.
25. Guobing, P. A. N., X. U. Fang, and C. H. E. N. Jiaoliao. "A novel algorithm for color similarity measurement and the application for bleeding detection in WCE." *International Journal of Image, Graphics and Signal Processing* 3.5 (2011): 1.